Parameter Study on the Formation of Macrosegregation in a Large Steel Ingot

L. Könözsy[1], F. Mayer[1], A. Ishmurzin[1], A. Kharicha[1], M. Wu[1], A. Ludwig[1],
R. Tanzer[2], W. Schützenhöfer[2]
[1] CD-Laboratory for Multiphase Modelling of Metallurgical Processes,
Department of Metallurgy, University of Leoben, A-8700 Leoben, Austria
[2] Böhler Edelstahl GmbH & Co KG, Kapfenberg, Austria

ABSTRACT: Investigations on the formation of macrosegregations are very important for the steel industry, since the mechanical properties depend strongly on the chemical composition and homogeneity. A parameter study for the solidification simulation of industrial scale steel ingots is performed with a recent multiphase volume averaging approach. This approach considers different phases (e.g. melt, columnar dendrite trunks and equiaxed grains), and solves the corresponding mass, momentum, energy conservation and species transport equations for each phase. The mass transfer between the phases is modelled by assuming diffusion controlled crystal growth. A hexagonal arrangement of the dendrite trunks is considered to compute the mass transfer during columnar solidification. The numerical model is implemented in the ANSYS-FLUENT commercial CFD software using User-Defined -Functions. The present paper focuses on the process parameters and their influence on the macrosegregation formation, namely the thermal and solutal expansion coefficients, and the parameters for modelling nucleation of equiaxed grains.

1. INTRODUCTION

Modeling of multicomponent solidification is a multiphase problem [1-5]. J. Gu and C. Beckermann used a model to study the multicomponent macrosegregation with numerical solution of fully coupled mass, momentum, energy and species conservation equations for the liquid and the solid regions as well as the mushy zone in the case of an industrial steel ingot [6]. The model was applied to investigate the macrosegregation and the flow field considering also thermal and solutal convection. The present work is a recent development and application of the volume averaged multiphase and multicomponent (Fe-C-Cr) model by A. Ludwig et. al. [7-9]. The model was validated in the case of a cast benchmark ingot by R. Tanzer et. al. [10] at the Böhler Edelstahl GmbH & Co KG (BEG) in Kapfenberg, Austria. The governing equations of the multiphase approach for solidification are presented. The numerical results are explained considering the process parameters such as the thermal and solutal convection and the nucleation parameters. This paper deals with results of our most recent volume averaged multiphase approach, applied to an industrial size ingot casting.

2. THE GOVERNING EQUATIONS AND MODEL DESCRIPTION

A volume averaged multiphase solidification model, which was developed for binary system [7-8], is currently extended for ternary system. Three phases are considered in the corresponding conservation equations, namely liquid phase l, columnar dendrite trunks c and globular-like equiaxed grains e. In order to define the mass transfer rates for the equiaxed and columnar phases, it is necessary to model their kinetic growth behaviour. The globular-like equiaxed crystals are assumed to be ideal spheres. Thus their growth velocity, assumed to be governed by diffusion, can be analytically derived [7-9] as

$$v_{R_e} = \frac{2D_j}{d_e} \cdot \frac{\widetilde{c}_l^{\,j} - c_l^j}{\widetilde{c}_l^{\,j} - \widetilde{c}_e^{\,j}}, \qquad (1)$$

where D_j is the diffusion coefficient of the j-th species in the liquid, d_e is the diameter of equiaxed grains, c_l^j is the liquid mass fraction of the j-th species, $\widetilde{c}_l^{\,j}$ and $\widetilde{c}_e^{\,j}$ are the equilibrium mass fractions at the liquid-solid interface. The j index is valid for all considered species in the multicomponent system (j =1 or 2 for ternary system).

Columnar dendrite trunks are approximated by growing cylinders. Their growth velocity, again assumed to be governed by diffusion, can be analytically derived [7-9] as

$$v_{R_c} = \frac{2D_j}{d_c} \cdot \frac{\tilde{c}_l^j - c_l^j}{\tilde{c}_l^j - \tilde{c}_c^j} \cdot \ln^{-1}\left(\frac{d_{\max}}{d_c}\right), \tag{2}$$

where $d_{\max}$ is the maximal diameter available for cylindrical growth, d_c is the actual diameter of columnar dendrite trunks, $\tilde{c}_c^j$ is the equilibrium mass fraction of the columnar solid at the liquid-solid interface. The maximal diameter can be chosen as $d_{\max} = 0.577 \cdot \lambda_1$ considering an hexagonal dendrite arrangement with dendrite arm spacing λ_1. This condition assumes that the entire residual melt is exactly consumed by the growing cylinder when they have reached its maximum diameter $d_{\max}$. When convection in the melt is strong, Eqs. (1)-(2) have to be modified by including the Sherwood number [9].

Knowing the growth velocity of the equiaxed grain from Eq. (1), the mass transfer rate from the liquid to equiaxed phase can be defined as

$$M_{le} = v_{R_e} \cdot \left(n \cdot \pi \cdot d_e^2\right) \cdot \rho_e \cdot f_{imp}, \tag{3}$$

which is the product of the growth velocity, the total surface area of spherical grains, the density of the equiaxed phase and the impingement factor for equiaxed growth. Also knowing growth velocity for columnar dendrite trunks from Eq. (2), the mass transfer rate from the liquid to columnar phase can be defined as

$$M_{lc} = v_{R_c} \cdot \left(\frac{2\sqrt{3} \cdot \pi \cdot d_c}{3\lambda_1^2}\right) \cdot \rho_c \cdot f_{imp}, \tag{4}$$

where ρ_c is the density of the columnar phase.

The impingement factors in Eqs. (3)-(4) are different for the spherical and cylindrical growth. For equiaxed solidification, the Avrami-type impingement factor is used ($f_{imp} = f_l$). For the definition of the columnar impingement factor, we assume a linear decrease with diameter for those trunks which have a larger diameter than the dendrite arm spacing.

$$f_{imp} = \begin{cases} 1, & 0 < d_c \le \lambda_1, \\ 1 - \dfrac{d_c - \lambda_1}{d_{\max} - \lambda_1}, & \lambda_1 < d_c \le d_{\max}, \end{cases} \tag{5}$$

The volume averaged and equilibrium mass fractions $c_l^j, \tilde{c}_l^j, \tilde{c}_e^j, \tilde{c}_c^j$ for the estimation of growth velocities are computed by solving a non-linear algebraic system of equations with a modified Newton-Raphson method. The process-related quantity c_l^j and the thermo-dynamic-related quantities $\tilde{c}_l^j, \tilde{c}_e^j, \tilde{c}_c^j$ are coupled with corresponding Fe-C-Cr phase diagram information [9].

After computing the mass transfer rates, the multiphase Eulerian-Eulerian approach is applied to consider the mass, momentum, enthalpy and species conservations. The conservation of mass for each phase is described by

$$\frac{D(f_l \rho_l)}{Dt} = -(M_{le} + M_{lc}), \tag{6}$$

$$\frac{D(f_e \rho_e)}{Dt} = M_{le}, \tag{7}$$

$$\frac{D(f_c \rho_c)}{Dt} = M_{lc}, \tag{8}$$

where f_i is the volume fraction of the corresponding phase, D/Dt is the substantial derivative. The mass transfer rate from the columnar to the equiaxed phase is neglected. The momentum conservation equation for the liquid phase is given by

$$\begin{aligned}\frac{D(f_l\rho_l\mathbf{u}_l)}{Dt} &= f_l\cdot\left\{\rho_l^{ref}+\rho_l^{ref}\cdot\left[\beta_T\left(T_l^{ref}-T_l\right)+\beta_c^j\left(c_l^{ref}-c_l^j\right)\right]\right\}\cdot\mathbf{g}-\nabla\cdot(f_l p)+\\ &+\nabla^2(\mu_l f_l\mathbf{u}_l)+\frac{1}{3}\nabla(\mu_l f_l\nabla\cdot\mathbf{u}_l)-\mathbf{u}_l(M_{le}+M_{lc})+K_{el}(\mathbf{u}_e-\mathbf{u}_l)+K_{cl}(\mathbf{u}_c-\mathbf{u}_l),\end{aligned} \tag{9}$$

where $\mathbf{u}_l,\mathbf{u}_e,\mathbf{u}_c$ are velocity vectors of the liquid, equiaxed and columnar phases, $\mathbf{g}$ is the gravity force, p is the scalar pressure field, μ_l is the dynamic viscosity of the liquid, K_{el},K_{cl} are drag coefficients among the phases. Thermal and solutal buoyancy are modelled by using the Boussinesq approach. $\rho_l^{ref},T_l^{ref},c_l^{ref}$ are the corresponding density, temperature and species reference values, β_T is thermal expansion coefficient and β_c^j is the solutal expansion coefficient of the j-th species. The momentum conservation equation for the equiaxed phase is given by

$$\begin{aligned}\frac{D(f_e\rho_e\mathbf{u}_e)}{Dt} &= f_e\cdot\{\rho_e+\Delta\rho_e\}\cdot\mathbf{g}-\nabla\cdot(f_e p)+\\ &+\nabla^2(\mu_e f_e\mathbf{u}_e)+\frac{1}{3}\nabla(\mu_e f_e\nabla\cdot\mathbf{u}_e)+\mathbf{u}_l M_{le}+K_{le}(\mathbf{u}_l-\mathbf{u}_e)+K_{ce}(\mathbf{u}_c-\mathbf{u}_e),\end{aligned} \tag{10}$$

where μ_e is the dynamic viscosity of equiaxed phase, $\Delta\rho_e$ is the density difference between the equiaxed and liquid phase, and K_{le},K_{ce} are the drag coefficients among the phases. The columnar dendrite trunks grow from the mould wall into the bulk melt and an advanced columnar tip front tracking method is applied for tracking the columnar tip envelop. The enthalpy conservation equations for the different phases are given by

$$\frac{D(f_l\rho_l h_l)}{Dt}=\nabla(f_l k_l\nabla T_l)-h_l(M_{le}+M_{lc})+H^*\cdot\left[(T_e-T_l)+(T_c-T_l)\right], \tag{11}$$

$$\frac{D(f_e\rho_e h_e)}{Dt}=\nabla(f_e k_e\nabla T_e)+h_e M_{le}+H^*\cdot\left[(T_l-T_e)+(T_c-T_e)\right], \tag{12}$$

$$\frac{D(f_c\rho_c h_c)}{Dt}=\nabla(f_c k_c\nabla T_c)+h_c M_{lc}+H^*\cdot\left[(T_l-T_c)+(T_e-T_c)\right], \tag{13}$$

where the enthalpies are defined as $h_l=\int_{T_{ref}}^{T_l}c_{p(l)}dT+h_l^{ref}$ and $h_e=h_c=\int_{T_{ref}}^{T_e}c_{p(s)}dT+h_e^{ref}$ with $c_{p(l)}$, $c_{p(s)}$ being the specific heat of the liquid and solid phase, and T_{ref} and h_l^{ref},h_e^{ref} are corresponding reference values. Note that the enthalpy differences between the liquid and solid phase, (h_l-h_e) and (h_l-h_c), define the latent heat of fusion. k_l,k_e,k_c are the thermal conductivities for each phase, H^* is the volumetric heat transfer coefficient between the phases, T_l,T_e,T_c are the corresponding temperatures of the phases, which are of course assumed to be equal. The species conservation equations for the different phases are given by

$$\frac{D\left(f_l \rho_l c_l^j\right)}{Dt} = -\tilde{c}_e^{\,j} M_{le} - \tilde{c}_c^{\,j} M_{lc}\,, \tag{14}$$

$$\frac{D\left(f_e \rho_e c_e^j\right)}{Dt} = \tilde{c}_e^{\,j} M_{le}\,, \tag{15}$$

$$\frac{D\left(f_c \rho_c c_c^j\right)}{Dt} = \tilde{c}_c^{\,j} M_{lc}\,, \tag{16}$$

where c_l^j, c_e^j, c_c^j are the mass fractions of the j-th species. In order to study the macrosegregation quantitatively, the mixture concentration is defined as

$$c_{mix}^j = \frac{c_l^j \cdot \rho_l^j \cdot f_l^j + c_e^j \cdot \rho_e^j \cdot f_e^j + c_c^j \cdot \rho_c^j \cdot f_c^j}{\rho_l^j \cdot f_l^j + \rho_e^j \cdot f_e^j + \rho_c^j \cdot f_c^j}\,. \tag{17}$$

The number density n of equiaxed grains is computed from

$$\frac{Dn}{Dt} = \frac{D(\Delta T)}{Dt} \cdot \frac{n_{\max}}{\sqrt{2\pi} \cdot \Delta T_\sigma} \cdot e^{-\frac{1}{2}\left(\frac{\Delta T - \Delta T_N}{\Delta T_\sigma}\right)^2}\,, \tag{18}$$

where $n_{\max}$ is the maximal available nucleation sites, ΔT is the constitutional undercooling, ΔT_N is the undercooling for maximum grain production rate and ΔT_σ is the Gaussian distribution width of the nucleation law. This approach, originally developed by W. Oldfield, suggests a continuous rather than a discrete distribution of nucleation sites [7].

The mass, momentum, energy and species conservation equations for each phases are solved numerically by Finite Volume Method (FVM) using FLUENT v6.3.

3. THE INDUSTRIAL STEEL INGOT

3.1 Experimental setup

The numerical model was applied for an industrial steel ingot with an approximate weight of 2 tons which was produced in the steel plant of BEG (Fig. 1). The material was melted in the electric arc furnace and cast into a grey cast mould which was instrumented with thermocouples at different heights and angles. To minimise the amount of shrinkage cavities at the top region of the ingot an insulation sleeve was used. The aim of this method is to assure that the top of the solidifying ingot stays liquid and thus keeping up its ability to feed the occurring shrinkage.

In order to compare the numerical predicted macrosegregations considering a ternary steel, a model alloy consisting of 0.38 wt.% Carbon and 16 wt.% Chromium was used for the ingot casting. The presence of trace elements in the chemical analysis (like Sulphur or Phosphorus) was negligibly small.

3.2 Boundary conditions

The boundary conditions for the energy conservation were estimated based on the experimental temperature measurements. The obtained value of 700 W/(m^{2}K) was used for the ingot/mould side walls and the bottom plate boundaries. The heat transfer coefficient at the top of the ingot was estimated to be 100 W/(m^{2}K) (Fig. 2.). For the flow field we used non-slip boundary conditions for both movable phases, liquid and equiaxed.

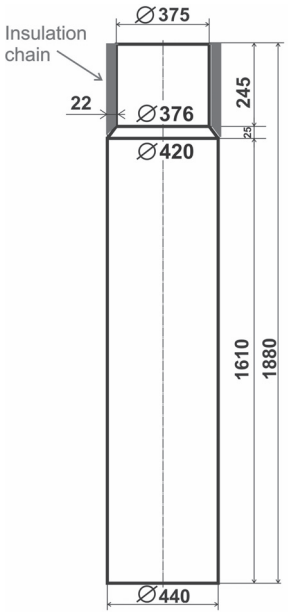

Fig. 1: Sketch of the industrial ingot

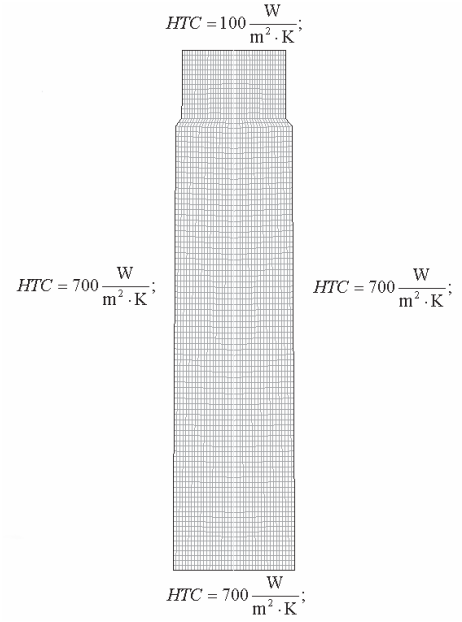

Fig. 2: The computational mesh and boundary conditions for the heat transfer coefficient

4. RESULTS AND DISCUSSION

As we do not consider any nucleation barrier for solidification at the mould wall, columnar dendrites start to grow from the mould wall towards the bulk melt as soon as the temperature decreases below the liquidus temperature. Simultaneously, equiaxed grains nucleate ahead of the columnar dendrite tips. As the solid density is larger than that of the melt, the equiaxed grains start to sink after having reached a certain size. On the other hand, thermal and solutal buoyancy may lead to a motion of melt ahead of the columnar dendrites or even within the interdendritic region. Whether the melt rises or sinks depends strongly on the value of the thermal and solutal expansion coefficients. The simulations presented in this paper were performed with β_T = 0.0002 K^{-1} for the thermal and β_c^C = -1.105 wt.%$^{-1}$ and β_c^{Cr} = 0.0 wt.%$^{-1}$ for the solutal expansion coefficients. Using these values, thermal buoyancy dominates and the melt at and in the columnar mush sinks. This leads to an overall downwards motion near the mould wall and thus an upwards motion in the centre of the ingot. The smaller equiaxed crystals follow this general flow pattern. Therefore, the simulations predict a chance of having smaller crystals flowing first downwards and then upwards again. However, these upwards flowing grains face high temperatures at the centre of the ingots and thus tend to melt again. Larger equiaxed grains sink more or less independent of the overall melt flow and hence finally settle at the bottom of the ingot. This grain sedimentation results in the well known cone-shaped equiaxed region at the ingot bottom. As consequence a cone-shaped region of negative macrosegregation forms (see Fig. 3-4).

Due to the fact that the three nucleation parameters, $n_{\max}$, ΔT_N and ΔT_σ (see Eq. (18)) are not known specifically for the ternary alloy of interest, we have varied them according to the values given in Table 2.

	$n_{\max}$	ΔT_N	ΔT_σ
(a)	7 ·10^9 m^{-3}	5 K	2 K
(b)	5 ·10^8 m^{-3}	6 K	3 K
(c)	7·10^9 m^{-3}	5 K	3 K

Tab. 2: Nucleation parameters used in the presented simulations

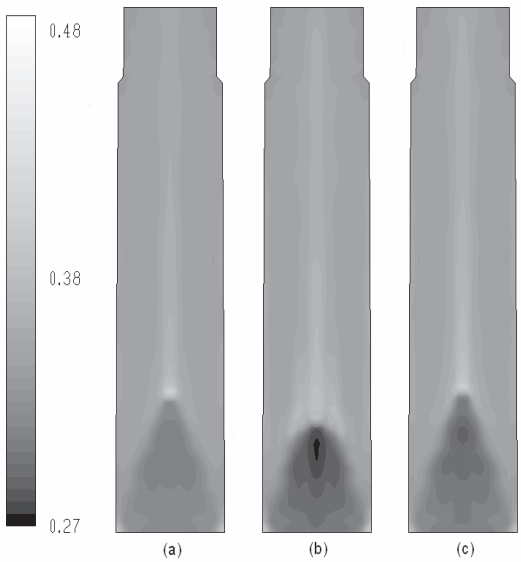

Fig. 3: Predicted distribution of Carbon-macrosegregation in wt.%

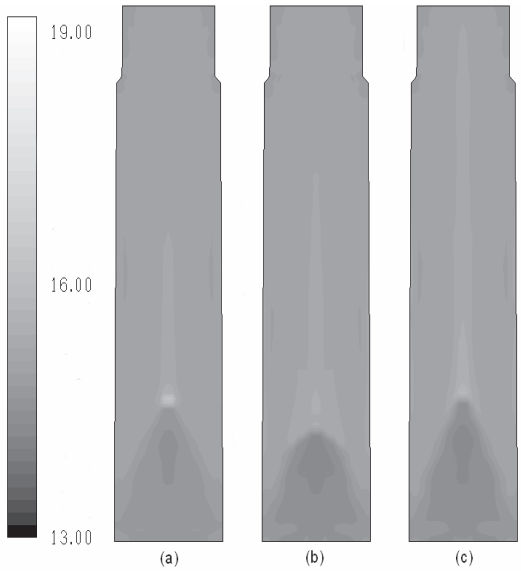

Fig. 4: Predicted distribution of Chromium-macrosegregation in wt.%

Fig. 3 and 4 show the predicted macrosegregation pattern of Carbon and Chromium for different nucleation parameters according to Tab. 2. The patterns for the two elements look similar although the orders of magnitude are different. For Carbon deviations from the initial composition by about ±25% and Chromium by about ±15% are predicted.

The study of the impact of different nucleation parameter shows that a broadening of a nucleation size distribution by increasing ΔT_σ leads to an augmentation of activated nuclei. The corresponding grains sediment and settle at the cone-shaped region forming an stronger negative segregated zone (see the stronger macrosegregation visible in Fig. 3 (c) compared to Fig. 3 (a)). Surprisingly, a reduction of the maximal available nucleation sites (decreased $n_{\max}$) and an increase of the undercooling for maximum grain production rate (increase ΔT_N) result in a stronger negative cone-shaped macrosegregation. During further proceeding of solidification, nucleation becomes more and more difficult and thus large areas of the elongated ingot solidify nearly completely with columnar dendritic microstructure. Here, a positive centre macrosegregation occur, as the ingot centre has the last (and therefore enriched) melt to solidify.

5. CONCLUSION AND OUTLOOK

An advanced volume averaged multiphase model to describe the columnar/equiaxed solidification of a ternary Fe-C-Cr alloy was presented and successfully applied to an industrial scale two tons ingot casting. Although key physical phenomena like nucleation, growth and sedimentation of equiaxed grains, fluid flow through columnar dendritic mush areas, thermal and solutal buoyancy, formation of micro- and macrosegregation etc. are addressed, the model lacks important material parameters. In this paper, we discussed the importance of the thermal and solutal expansion coefficients and the three nucleation parameter for the formation of overall convection during solidification and with that, for the formation of macrosegregations. The comparison of numerically predicted macrosegregations with measurements will be discussed in a future paper.

6. ACKNOWLEDGEMENT

This work is financially supported by the Austrian Christian-Doppler Research Society, and Boehler Edelstahl GmbH & Co KG for which the authors kindly acknowledge. The authors wish to express their appreciation to ANSYS Inc./FLUENT Inc. for their technical assistance.

7. REFERENCES

[1] M.C. Flemings: Solidification Processing, McGraw-Hill, New York, (1974).

[2] K. Miyazawa, K. Schwerdtfeger, Arch. Eisenhüttenwes., 52 (1981) pp. 415–422.

[3] G. Lesoult, S. Sella, Proc. 6th Internat. Iron and Steel Congress, Nagoya, Iron and Steel Institute of Japan, vol. 1 (1990) pp. 681–688.

[4] Wang, C.Y. and Beckermann, C., Metall. Trans., 24A (1993) p. 2787.

[5] Wang, C.Y. and Beckermann, C., Metall. Mater. Trans., 27A (1996) p. 2754.

[6] J.P. Gu, C. Beckermann, Metall. Mater. Trans., 30A (1999) pp. 1357-1366.

[7] A. Ludwig, M. Wu, Mat. Sci. Eng. A413-414 (2005) pp. 109-114.

[8] M. Wu and A. Ludwig, Metall. Mater. Trans., 37A (2006) pp. 1613-1631.

[9] A. Ludwig, A. Ishmurzin, M. Gruber-Pretzler, F. Mayer, M. Wu, R. Tanzer., W. Schützenhöfer, Proceedings of the 5th Decennial Int. Conf. on Solidification Processing, Sheffield, UK (2007) pp. 493-496.

[10] R. Tanzer, W. Schützenhöfer, G. Reiter, H.-P. Fauland, L. Könözsy, A. Ishmurzin, M. Wu, A. Ludwig, “The Validation of a Multiphase Model for the Macrosegregations and Primary Structure of High Grade Steel Ingots”, LMPC’2007 Int. Conf., to be held in Nancy, France, (2007).